Journal of Applied Mechanics and Technical Physics, Vol. 51, No. 2, pp. 202–210, 2010

FLOW STRUCTURE AT THE INITIAL SECTION OF A SUPERSONIC JET EXHAUSTING FROM A NOZZLE WITH CHEVRONS

V. I. Zapryagaev, I. N. Kavun, and N. P. Kiselev

UDC 533.6.011.5

The spatial structure of the flow in a supersonic underexpanded jet exhausting from a convergent nozzle with vortex generators (chevrons) at the exit is experimentally studied. Exhaustion of a supersonic underexpanded jet from a nozzle with chevrons at the nozzle exit is numerically simulated with the use of the Fluent commercial software package. The experimental and numerical data are demonstrated to be in reasonable agreement. The influence of chevrons on the process of gas mixing is estimated.

Key words: *supersonic underexpanded jet, vortex generators, chevron, tab.*

Introduction. Studying the mixing processes in a supersonic jet containing artificial disturbances is an important scientific problem. Such disturbances are generated by various devices, such as tabs, chevrons, corrugated surfaces, lobed mixers, etc.; chevrons and tabs are used both to intensify the mixing process and to reduce the level of noise generated by the jet.

Zapryagaev and Solotchin [1] performed experiments in a nozzle without artificial disturbances and found that there are azimuthal inhomogeneities of the distributions of gas-dynamic quantities (pressure and density) in the shear layer of a supersonic jet. It was shown that the origin of azimuthal inhomogeneities is caused by the presence of streamwise vortex structures of the Taylor–Görtler type [2]. One of the governing factors of the emergence of vortex structures in supersonic underexpanded jets is the curvature of streamlines [3]. The use of various vortex-forming elements at the nozzle exit leads to significant reconstruction of the jet flow and to formation of large-scale streamwise vortices in both supersonic and subsonic flows [4–6]. Artificial streamwise vortices intensify the process of gas mixing and reduce the level of noise generated by the jet [6, 7].

A tab is a projection (flap) located on the surface wetted by a gas or a liquid and acting on the flow by means of changing the flow structure [6]. A chevron is a vortex-forming element (vortex generator) shaped as a triangle (or a trapezium) whose inner surface is a continuation of the inner surface of the nozzle exit (Fig. 1) [8]. These definitions are applicable to the vortex generator at the nozzle exit with exhaustion of a supersonic jet, because the character of flow interaction with the vortex generator depends on the exhaustion regime (pressure ratio at the nozzle exit).

The use of chevrons and tabs in nozzles of turbofan engines allows the jet noise to be substantially reduced. Optimal configurations of nozzles with chevrons and tabs were found, which made it possible to reduce the noise level by 2.7 dB with a minor loss in thrust (approximately 0.06%) [8].

In addition to experimental research, numerical and theoretical methods of studying turbulent jet noise are developed. Shur et al. [9] used large eddy simulations to study the mechanisms of noise generation and propagation in transonic and supersonic jets at high Reynolds numbers and also the formation of acoustic waves in complex jets exhausting from bypass nozzles and from nozzles with the central body. As a result, integral characteristics of the flow (thrust and flow rate) were obtained, and the influence of vortex generators on the noise level of the jet was studied.

Khristianovich Institute of Theoretical and Applied Mechanics, Siberian Division, Russian Academy of Sciences, Novosibirsk, 630090; nkiselev@itam.nsc.ru. Translated from Prikladnaya Mekhanika i Tekhnicheskaya Fizika, Vol. 51, No. 2, pp. 71–80, March–April, 2010. Original article submitted February 9, 2009; revision submitted March 16, 2009.

Fig. 1. Nozzle with chevrons.

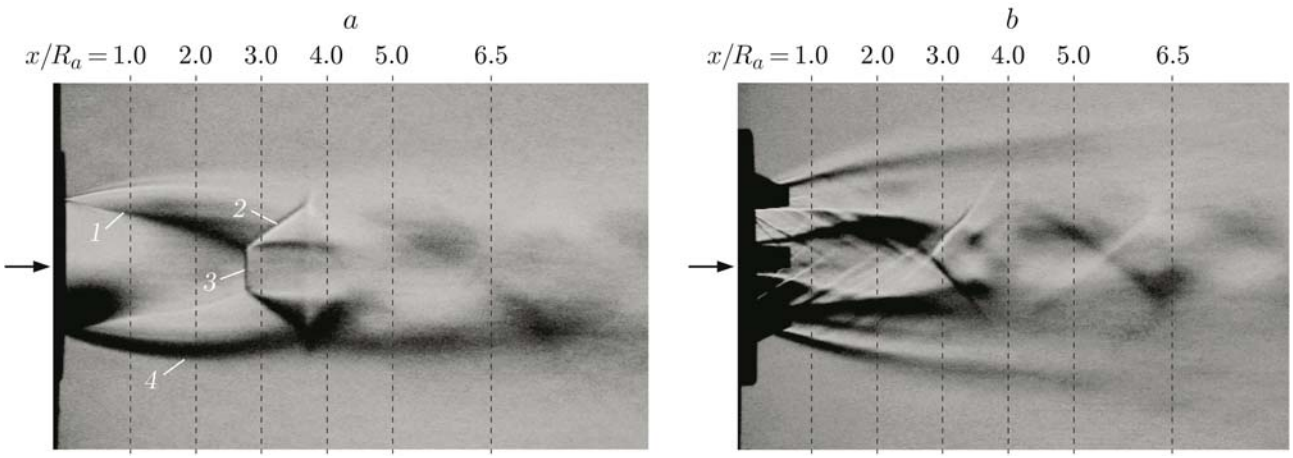

Fig. 2. Schlieren pictures of a supersonic underexpanded jet ($M_a = 1.0$ and $n_p = 2.64$) exhausting from a "clear" nozzle (a) and from a nozzle with chevrons at the exit (b): 1) barrel shock wave; 2) reflected shock wave; 3) Mach disk; 4) jet boundary; the arrows indicate the flow direction.

The flow structure in supersonic jets with large-scale streamwise vortices generated by vortex-forming elements, such as chevrons and tabs, has not been adequately examined. The objective of the present activities was an experimental and numerical study of the gas-dynamic flow structure at the initial section of a supersonic underexpanded jet exhausting from the nozzle with six vortex-forming elements in the form of chevrons at the nozzle exit. The influence of chevrons on the mixing process at the initial section of the jet was estimated by using numerical data.

Experimental Technique and Data. The experimental study was performed in a jet module of a T-326 hypersonic wind tunnel based at the Khristianovich Institute of Theoretical and Applied Mechanics of the Siberian Division of the Russian Academy of Sciences. The Mach number at the nozzle exit was $M_a = 1.0$ and the nozzle pressure ratio was $n_p = P_a/P_c = 2.64$ (P_a is the pressure at the nozzle exit and P_c is the pressure in the working chamber of the facility). The supersonic jet exhausted into an ambient space (air) from an axisymmetric convergent contoured nozzle with $M_a = 1$, which was equipped with six chevrons on a cylindrical insert at the exit. A constant pressure ratio $N_{pr} = P_0/P_c = 5$ (P_0 is the pressure in the settling chamber of the jet module) was maintained during the experiment; the Reynolds number calculated on the basis of the nozzle-exit diameter was $Re_d = 2.3 \cdot 10^6$. The radius of the nozzle exit and the insert with chevrons was $R_a = 15$ mm. The chevrons were aligned with an identical step over the azimuth and were shaped as trapezoids with a height of 10 mm and base lengths of 7 and 4.5 mm. The generatrix of the inner surface of the chevron was a continuation of the inner surface of the nozzle exit.

Figure 2 shows the schlieren pictures of the initial section of a supersonic underexpanded jet exhausting from a "clear" nozzle and from a nozzle with chevrons at the exit, which were obtained by an optical visualization system consisting of an IAB-451 shadowgraph and a digital camera with a resolution of 640×480 pixels.

Detailed measurements of the pressure distribution $P_t(r, \varphi)$ (r and φ are the radial and azimuthal coordinates) were performed in several cross sections of the supersonic jet by a total pressure probe (Pitot tube) with an outer diameter of 0.6 mm. An automated system of data acquisition and processing was used to obtain the pressure fields. The total pressure probe was moved by an automated traversing gear in three directions: along

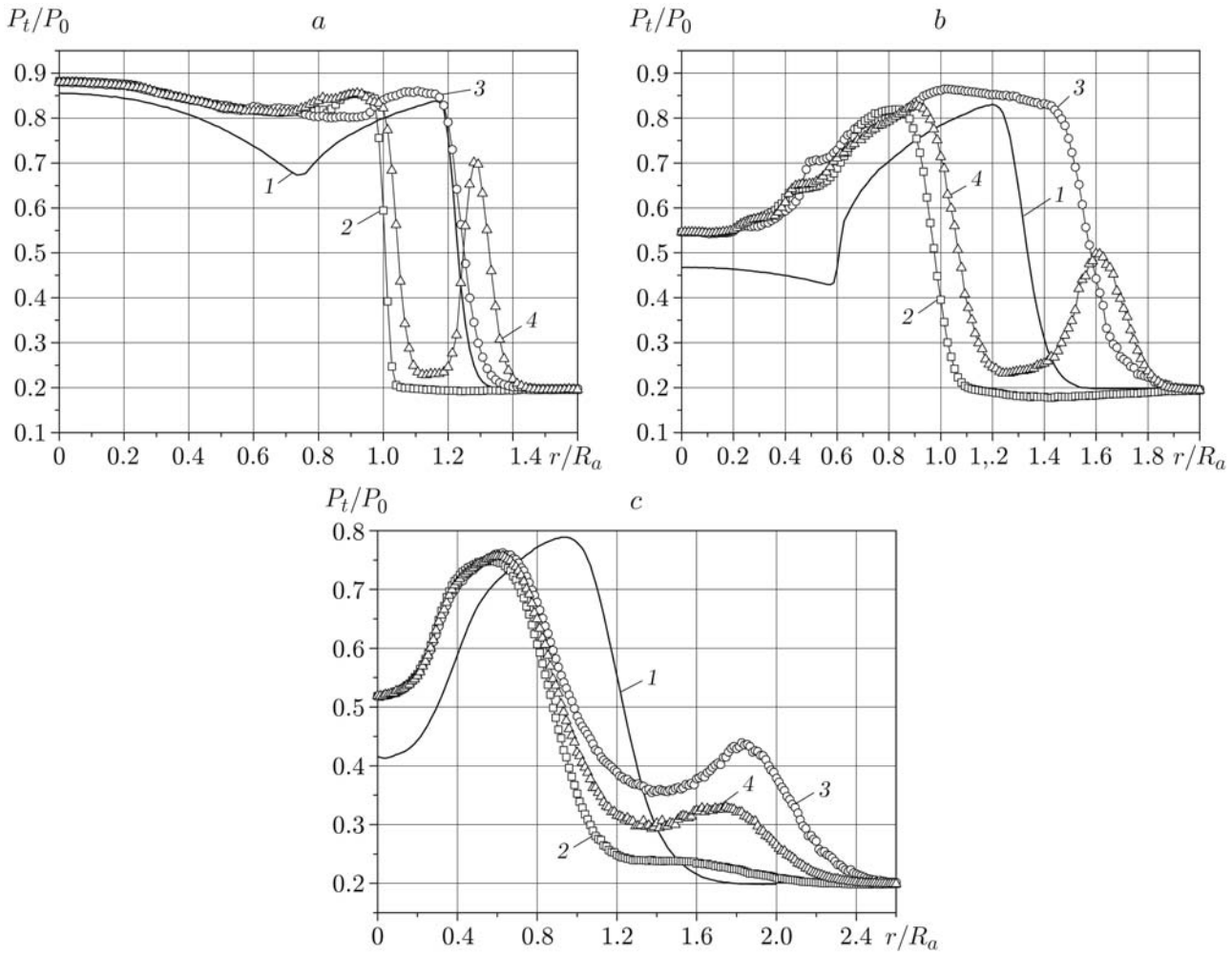

Fig. 3. Radial profiles of pressure measured in different sections of the jet: $x/R_a = 1$ (a), 2 (b), and 5 (c); curve 1 refer to the jet exhausting from a "clear" nozzle and curves 2–4 refer to the jet exhausting from a nozzle with chevrons for different positions of the Pitot tube corresponding to the radial displacement lines: with respect to the chevron axis ($\varphi = 0^\circ$) (2) and between two neighboring chevrons at $\varphi = 30^\circ$ (3) and at 15° (4).

the streamwise x, transverse (r), and azimuthal φ coordinates. The radial and azimuthal pressure profiles were obtained in the jet cross sections $x/R_a = 1.0$, 2.0, 3.0, 4.0, 5.0, and 6.5 (see Fig. 2).

A typical shock-wave structure is formed in a free supersonic underexpanded jet (see Fig. 2a). This shock-wave structure includes the barrel shock wave, the reflected shock wave, the Mach disk, and the jet boundary. The flow pattern in the jet exhausting from a nozzle with chevrons (see Fig. 2b) is more complicated: the jet boundary is smeared and the chevrons interact with the supersonic jet flow, which leads to generation of shock waves interacting with each other and intersecting on the jet axis.

Typical radial profiles of pressure in different sections of the jet are shown in Fig. 3.

In the case of a "clear" jet, there is a pressure jump at $r/R_a = 0.6$ and $x/R_a = 2.0$ (see Fig. 3b), which corresponds to the location of the barrel shock wave; the pressure maximum $P_t/P_0 = 0.825$ ($r/R_a = 1.2$) corresponds to the inner boundary of the shear layer of the jet, and the pressure minimum $P_t/P_0 = 0.2$ ($r/R_a = 1.6$) corresponds to the outer boundary of the jet.

The presence of chevrons exerts a significant effect on the flow structure in the underexpanded jet. Wavy variations of pressure are observed in the inner flow region ($0.2 < r/R_a < 0.8$) (see Fig. 3b) due to the presence of shock waves formed owing to jet interaction with the chevrons and intersecting on the axis. The pressure on the jet axis is higher in the undisturbed jet ($P_t/P_0 = 0.55$ for the nozzle with chevrons and $P_t/P_0 = 0.47$ for the

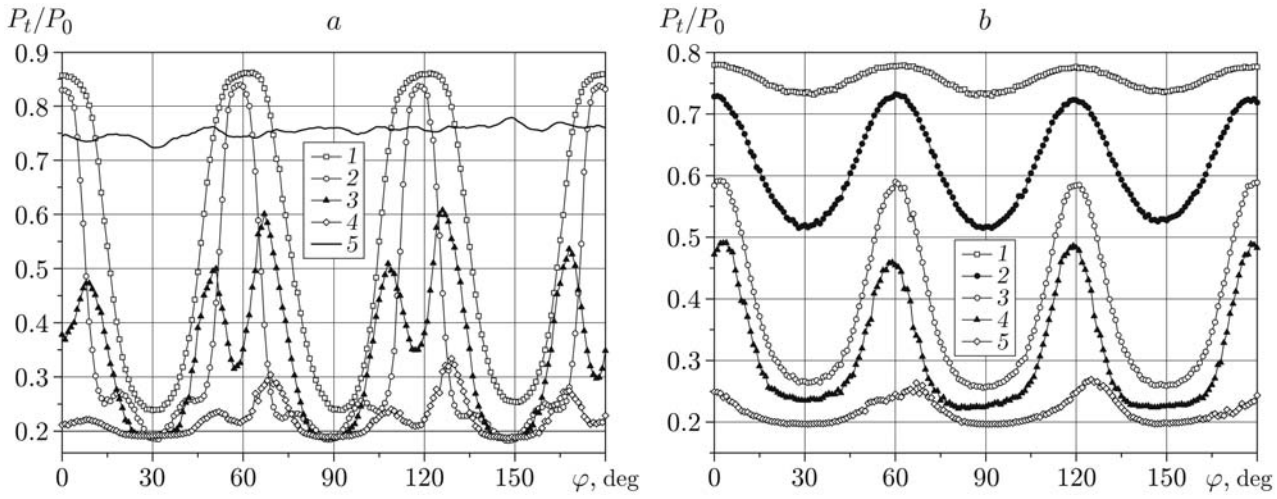

Fig. 4. Azimuthal distributions of the normalized pressure measured in different cross sections of the jet: (a) $x/R_a = 2.0$ and $r/R_a = 1.0$ (1), 1.27 (2), 1.6 (3), 1.73 (4), and 1.27 (undisturbed jet) (5); (b) $x/R_a = 4.0$ and $r/R_a = 0.67$ (1), 0.8 (2), 1.0 (3), 1.27 (4), and 2.13 (5).

smooth nozzle). The inner boundaries of the shear layer behind the chevron ($\varphi = 0°$ and $r/R_a = 0.83$) and $\varphi = 15°$ ($r/R_a = 0.90$) are shifted toward the axis, as compared with the undisturbed jet, whereas the inner boundary between the chevrons ($\varphi = 30°$) is shifted away from the axis ($r/R_a = 1.4$). The outer boundary of the jet located between the neighboring chevrons (curves 3 in Fig. 3) is also shifted away from the axis ($r/R_a = 1.88$); therefore, the transverse size of the jet increases. At $\varphi = 0°$ (curves 2), the outer boundary of the jet is shifted toward the axis ($r/R_a = 1.1$), which indicates considerable deformation of the boundary caused by an inflow of a low-pressure gas from the ambient space. At $\varphi = 15°$ (curve 4 in Fig. 3b), $r/R_a = 1.6$, there is an additional pressure peak ($P_t/P_0 = 0.5$); the mechanism of its origination is described below. The barrel shock wave is not observed in the jet exhausting from the nozzle with chevrons, which testified to significant changes in the shock-wave structure of the supersonic jet.

With distance from the nozzle exit (see Fig. 3c), the inner boundary of the shear layer is shifted toward the axis, as compared with the situation of the undisturbed flow, whereas the outer boundary is shifted away from the axis. The radial pressure distributions in other streamwise sections of the initial section of the jet correspond to the radial profiles shown in Fig. 3.

As a result of interaction of the chevrons with the supersonic jet flow, a complicated shock-wave structure is formed at the initial section of the jet, and additional shock waves interacting with each other appear.

Figure 4 shows the typical azimuthal profiles of the normalized pressure in the jet sections $x/R_a = 2$ and 4. The measurements were performed in the range of the angles $\varphi = 0$–360°; for better presentation of the spatial flow in the shear layer of the jet, however, Fig. 4 shows the data obtained at $\varphi = 0$–180°.

In the "clear" jet (curve 5 in Fig. 4a), there are azimuthal inhomogeneities of pressure owing to natural roughness on the inner surface of the nozzle and streamwise Taylor–Görtler vortices. Streamwise vortices can be formed if the streamlines in the shear layer of the jet are curved owing to hydrodynamic instability of the shear layer caused by additional centrifugal forces. The small magnitude of the azimuthal inhomogeneities of pressure is caused by small initial perturbations in the shear layer of the jet; the magnitude of these initial perturbations is determined by the quality of machining of the inner surface of the nozzle. In the case considered here, the measured roughness of the inner surface of the nozzle was 0.25 μm.

The chevrons induce significant transformations of the azimuthal profiles. The minimum values of pressure are registered at the values of φ corresponding to the flow in the wake behind the chevron. The minimum values of pressure are commensurable with the pressure in the working chamber of the jet module. In addition to the principal minimums, there appear additional pressure maximums on the outer boundary of the jet (curve 3 in Fig. 4a); the values of these maximums are comparable with the values of the minimums. The magnitude of the maximums decreases with a further increase in the radius (curve 4 in Fig. 4a). The emergence of the minimums

and maximums is caused by large-scale streamwise vortices resulting from interaction of the chevrons with the supersonic jet flow.

Figure 5 shows the experimentally measured azimuthal distributions of the Pitot pressure in different cross sections of the jet exhausting from the nozzle with the chevrons. Thirty to thirty eight azimuthal distributions of pressure were obtained in each cross section. Thus, the results measured at 10,800–13,600 points were used to construct the flow topology in each cross section of the jet. The azimuthal angles $\varphi = 0$, 15, and 30° shown in Fig. 5b correspond to the radial lines on which the pressure profiles shown in Fig. 3 were obtained. The numbers 1–4 indicate the radii at which the azimuthal pressure profiles in Fig. 4a were obtained.

The resultant flow structure is induced by formation of large-scale vortex structures owing to interaction of the chevrons with the jet boundary. Each chevron generates a pair of oppositely rotating streamwise vortices. It is seen that the vortex structures have a mushroom shape. The process of generation, evolution, and dissipation of artificially induced mushroom-shaped disturbances is clearly traced. The generation is observed at $x/R_a = 1$, the evolution occurs at $x/R_a = 2$–3, and the dissipation is observed at $x/R_a = 6.5$. The vortex flow behind the chevron ($\varphi = 0°$) is directed so that the low-pressure gas enters the jet in the radial direction (see Fig. 5b). In the region between the neighboring chevrons ($\varphi = 30°$), the high-pressure gas is entrained to the jet periphery.

The emergence of the secondary pressure maximum at $r/R_a = 1.6$ and $\varphi = 15°$ (see Fig. 3b) can be explained by using isobars in the jet cross section (curve 3 in Fig. 5b). A high-pressure reverse vortex flow directed toward the jet axis is registered at $\varphi = 15°$ and $r/R_a = 1.6$.

With distance from the nozzle exit ($x/R_a = 5.0$ and 6.5), the ordered flow structure becomes smeared, the vortex flow intensity decreases, the "stems" of the mushroom-shaped structures become thinner, the pressure decreases, and the vortex is separated from the jet core (see Fig. 5f). It should be noted that the mushroom-shaped structures exist at a rather large distance from the nozzle exit.

Subsonic flows also display mushroom-shaped vortex structures. For instance, Litvinenko et al. [10] used visualization in experiments with a subsonic jet in the presence of ordered roughness on the inner surface of the nozzle and acoustic disturbances of specified frequency. The streamwise vortex structures were observed to interact in the shear layer with crossflow Kelvin–Helmholtz vortices, which results in the formation of three-dimensional Λ-structures forming mushroom-shaped disturbances on the outer boundary of the jet.

Numerical Calculations. A numerical study was performed for the purposes of verification of the Fluent software package for the case of exhaustion of a supersonic nonisobaric jet and also obtaining quantitative data on the gas-dynamic structure of a supersonic jet in the presence of vortex-forming devices (tabs or chevrons) at the nozzle exit. Three-dimensional Navier–Stokes equations were solved with the use of the k–ε turbulence model.

The calculations were performed for a nozzle with the exit radius $R_a = 15$ mm and six chevrons at the exit (see Fig. 1). The Mach number at the nozzle exit was $\mathrm{M}_a = 1$, the nozzle pressure ratio was $n_p = 2.64$, and the Reynolds number based on the nozzle-exit diameter d was $\mathrm{Re}_d = 2.3 \cdot 10^6$. The computational domain is a segment whose size is 1/12 of a cylinder of length $x/R_a = 5.0$ and radius $r/R_a = 3.33$. The side planes of the segment are planes of symmetry of the problem; one of them passes through the middle of the chevron, and the other is at an identical distance from the neighboring chevrons. The number of cells in the computational domain is approximately 0.5 million.

To estimate the reliability, the calculated data were compared with the results of an experiment performed under the same geometric and gas-dynamic conditions. Figure 6 shows the radial distributions of the pressure P_t/P_0 in the jet cross section $x/R_a = 1$ at different values of the angle φ. The pressure distributions along the radial line passing through the middle of the chevron at $\varphi = 0°$ (see Fig. 6a), along the line at $\varphi = 15°$ (see Fig. 6b), and along the line passing at an identical distance between the neighboring chevrons at $\varphi = 30°$ (see Fig. 6c) are plotted. As the total pressure is measured by a Pitot tube in the experiment, the numerical data have to be converted to a form suitable for comparisons with the experimental results. The calculated static pressure p and the local Mach number M_x in the x direction were used to recalculate the pressure distributions P_t/P_0 by the formulas given in [11]:

$$\frac{P_t}{P_0} = \begin{cases} \dfrac{p}{P_0}\Big(1 + \dfrac{k-1}{2}\,\mathrm{M}_x^2\Big)^{k/(k-1)}, & \mathrm{M}_x < 1, \\ \dfrac{p}{P_0}\Big(\dfrac{2k}{k+1}\,\mathrm{M}_x^2 - \dfrac{k-1}{k+1}\Big)\Big(\dfrac{4k}{(k+1)^2} - \dfrac{2(k-1)}{(k+1)^2\mathrm{M}_x^2}\Big)^{-k/(k-1)}, & \mathrm{M}_x \geqslant 1 \end{cases} \tag{1}$$

(k is the ratio of specific heats of air).

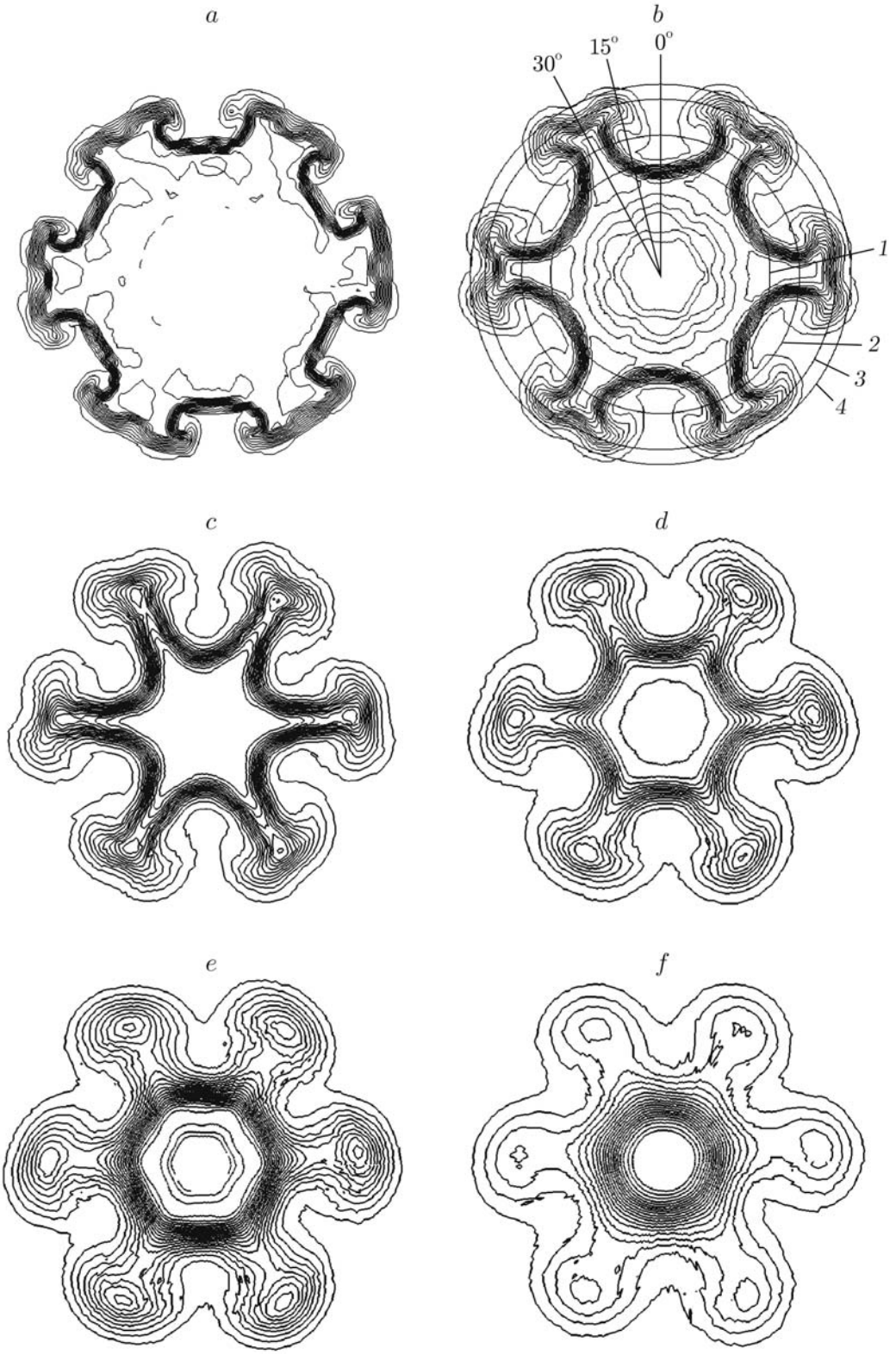

Fig. 5. Contours of pressure measured in different cross sections of the jet: $x/R_a = 1.0$ (a), 2.0 (b), 3.0 (c), 4.0 (d), 5.0 (e), and 6.5 (f); $r/R_a = 1.00$ (1), 1.27 (2), 1.60 (3), and 1.73 (4).

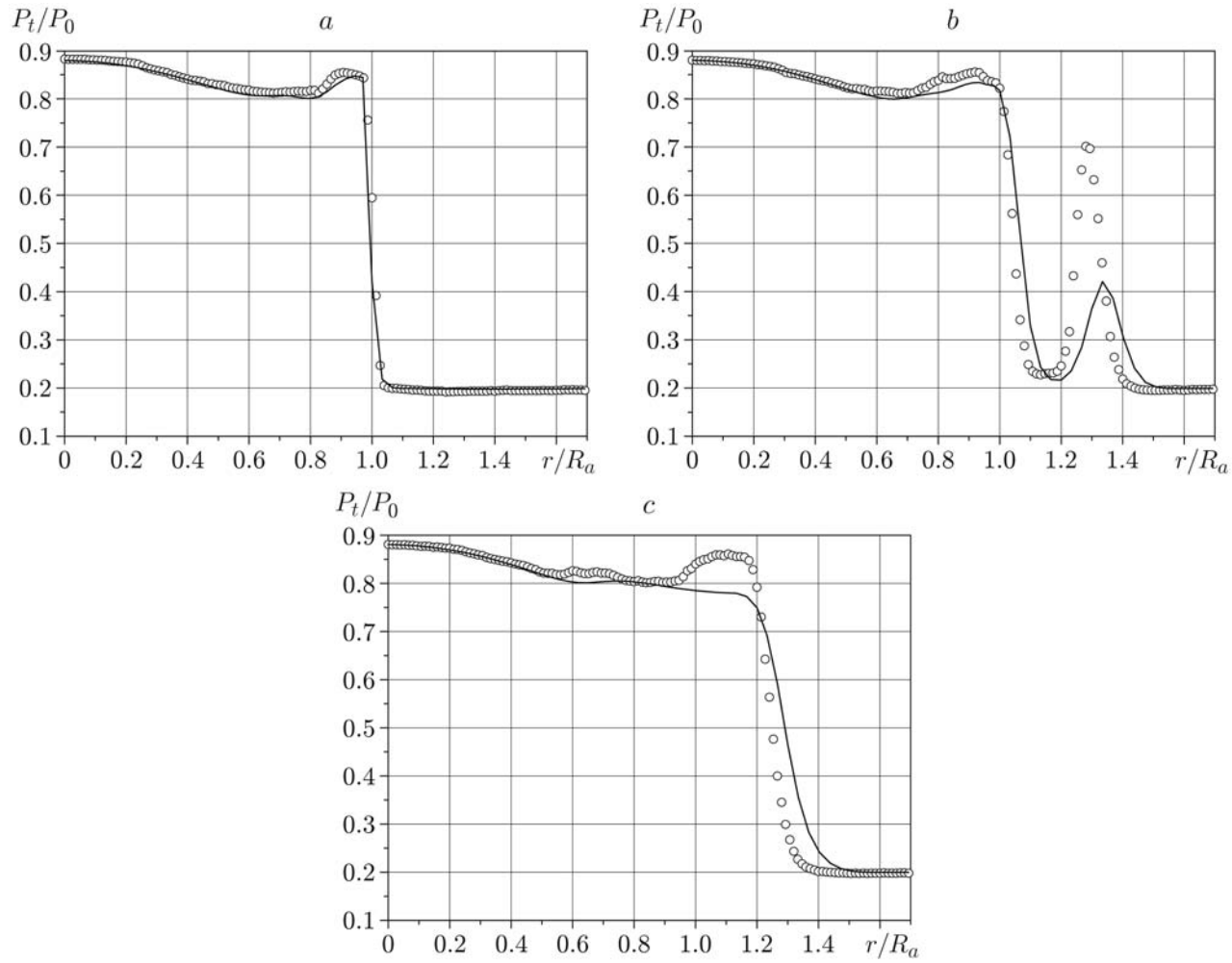

Fig. 6. Radial profiles of pressure in the jet cross section $x/R_a = 1.0$ at $\varphi = 0^\circ$ (a), 15° (b), and 30° (c); the curves and points are the results calculated by Eqs. (1) and obtained in experiments, respectively.

It is seen in Fig. 6 that the experimental and calculated data are in reasonable agreement. The greatest difference is observed at $\varphi = 15^\circ$ and $r/R_a = 1.3$ (see Fig. 6b) corresponding to the secondary maximum of pressure. The calculated and measured values of pressure in the flow core are in good agreement. The agreement in the shear layer of the jet is only qualitative, because the turbulence model used in the calculations allowed us to obtain a qualitative description of the real flow structure, but could not reproduce all elements of the flow.

Figure 7 shows the streamlines constructed on the basis of the radial and azimuthal components of the velocity vector in the jet cross section $x/R_a = 3$. It is seen that each chevron generates a pair of vortices formed near the side surface of the chevron and propagating in the downstream direction. The flow has a mushroom-shaped structure and consists of six paired vortices, which agrees qualitatively with the experimental data (see Fig. 5). The transverse sizes of the vortices increase with distance from the nozzle exit, and their intensity decreases.

Based on our calculations, we obtained the mass flow G in the cross section x/R_a for the gas exhausting from a "clear" nozzle and from a nozzle with chevrons:

$$G(x/R_a) = \int\limits_s \rho V_x \, ds.$$

Here, ρ is the gas density, V_x is the axial component of the velocity vector, and s is the cross-sectional area of the computational domain. The mass flow in the cross section of the computational domain for the jet exhausting from the nozzle with chevrons is found to increase linearly with increasing streamwise distance and to exceed the corresponding value for the undisturbed jet approximately by 20% (at $x/R_a = 5$).

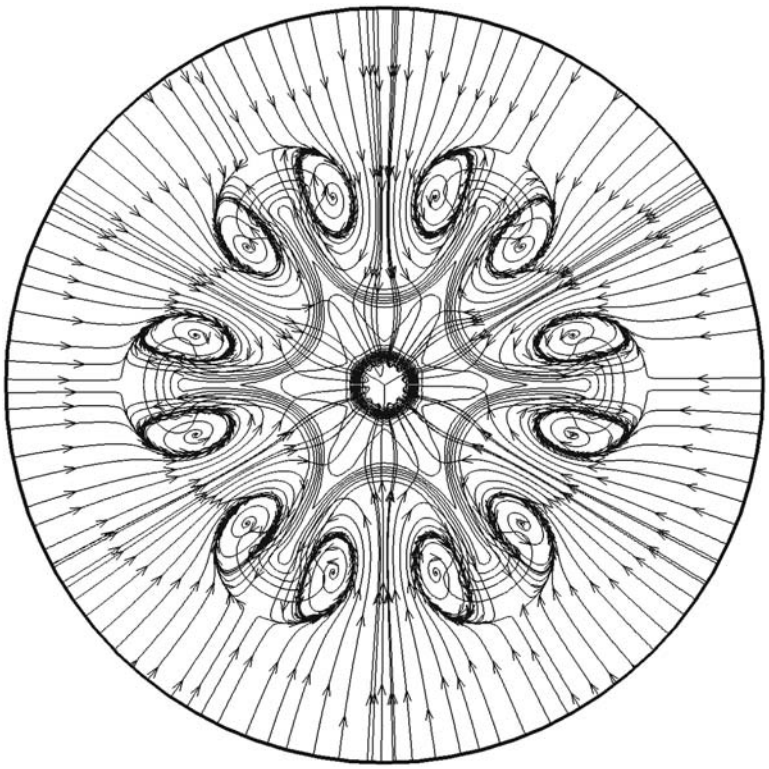

Fig. 7. Streamline constructed on the basis of the radial and azimuthal components of the velocity vector in the jet section $x/R_a = 3$.

Conclusions. The flow structure in a supersonic axisymmetric underexpanded jet exhausting from a convergent nozzle with six chevrons at the exit is studied. Interaction of the chevrons with the jet flow leads to transformation of the stationary jet structure and to formation of mushroom-shaped large-scale vortex structures. Numerical simulations of the supersonic underexpanded jet exhausting from the nozzle with chevrons allowed us to determine the structure of the streamwise vortices generated by the vortex-forming element and also to find the specific features of formation of the mushroom-shaped structures in the shear layer. The secondary maximum in the radial distribution of the measured Pitot pressure at the jet boundary is caused by the deflection of the high-pressure gas flow direction (toward the jet axis). Numerical predictions show that the chevrons increase the shear layer thickness by 20% at a distance $x/R_a = 5$.

This work was supported by the Russian Foundation for Basic Research (Grant No. 09-08-00165) and by the Siberian Supercomputer Center of the Siberian Division of the Russian Academy of Sciences.

REFERENCES

1. V. I. Zapryagaev and A. V. Solotchin, "Spatial structure of the flow in the initial section of a supersonic underexpanded jet," Preprint No. 23–88, Inst. Theor. Appl. Mech., Sib. Div., Acad. of Sci. of the USSR, Novosibirsk (1988).
2. V. I. Zapryagaev and A. V. Solotchin, "Three-dimensional structure of flow in a supersonic underexpanded jet," *J. Appl. Mech. Tech. Phys.*, **32**, No. 4, 503–507 (1991).
3. V. I. Zapryagaev, N. P. Kiselev, and A. A. Pavlov, "Effect of streamline curvature on intensity of streamwise vortices in the mixing layer of supersonic jets," *J. Appl. Mech. Tech. Phys.*, **45**, No. 3, 335–343 (2004).
4. A. Krothapalli, G. Buzyna, and L. Lourenco, "Streamwise vortices in an underexpanded axisymmetric jet," *Phys. Fluids, A*, **3**, No. 8, 1848–1851 (1991).

5. D. C. MacCormic and J. C. Bennett (Jr.), "Vortical and turbulent structure of a lobed mixer free shear layer," *AIAA J.*, **32**, No. 9, 1852–1859 (1994).
6. M. Samimy, K. B. M. Q. Zaman, and M. F. Reeder, "Effects of tabs on the flow and noise field of an axisymmetric jet," *AIAA J.*, **31**, No. 4, 609–619 (1993).
7. K. M. Khritov, V. Ye. Kozlov, S. Yu. Krasheninnikov, et al., "On the prediction of turbulent jet noise using traditional aeroacoustic methods," *J. Aeroacoustic*, **4**, Nos. 3/4, 289–324 (2005).
8. N. Sayed, K. Mikkelsen, and J. Bridges, "Acoustics and thrust of quiet separate-flow high-bypass-ratio nozzles," *AIAA J.*, **41**, No. 3, 372–378 (2003).
9. M. R. Shur, F. R. Spalart, and M. Kh. Strelets, "Calculation of noise of complex jets on the basis of the first principles," *Mat. Model.*, **19**, No. 7, 5–26 (2007).
10. M. V. Litvinenko, V. V. Kozlov, G. V. Kozlov, and G. R. Grek, "Effect of streamwise streaky structures on turbulization of a circular jet," *J. Appl. Mech. Tech. Phys.*, **45**, No. 3, 349–357 (2004).
11. A. N. Petunin, *Methods and Techniques of Measuring of Gas Flow Parameters* [in Russian], Mashinostroenie, Moscow (1972).